Sample Rate Selection for Aircraft Digital Control

J. David Powell*
Stanford University, Stanford, Calif.

and

Paul Katz†
Ministry of Defense, Haifa, Israel

The identification and evaluation of the important considerations in selecting sample rates for aircraft digital control systems are discussed. The design method used in the evaluation is a discrete optimal synthesis technique which possesses no artificial sample rate constraints due to discretization approximations. As an illustration of the sample rate selection criteria, the methods were applied to a specific longitudinal design including wind gusts and a bending mode. The dominant limitations on the sample rate were found to be the transient response characteristics and the response due to wind disturbances. Stabilization of the bending mode was not a limiting factor on the sample rate, although it was necessary to desensitize the design for acceptable performance with imperfect knowledge of the bending mode frequency. It appears that a sample rate between 10 and 20 Hz would be adequate for this example.

I. Introduction

AIRCRAFT digital control systems have now been implemented[1,2] and many more have been studied.[3-7] In any aerospace digital autopilot design process, the sample rate must be selected and the literature discusses various methods of accomplishing this selection. Sample rate selection is sometimes based on a certain multiple of the highest important bending mode. An appropriate value for this multiple was reported by Lee[7] to be four. Others[8-10] have also selected sample rates to be about four times the highest important bending mode; however, it is perhaps more typical to select sample rates at approximately six to ten times the highest bending mode.[1,3,4,6,11] Recently, Berman[5] introduced the concept that the proper sample rate is independent of the bending modes and should be based solely on disturbance effects. This was applied to a V/STOL example and yielded a sample rate which was slower than the highest bending mode. The purpose of this paper is to bring the different (and sometimes divergent) techniques together, to show the applicability of each, and to offer some alternate criteria which are more directly related to the actual sample rate effects.

The design technique used in the analysis often influences the sample rate selection and, in some cases, causes the sample rate to be significantly faster than required. Although many variations exist, we prefer to divide the design methods into two broad categories: 1) those where the design is done in the continuous domain (or s-plane); and 2) those where the design is done in the discrete domain (z or w-plane). Design using the first category is attractive since it utilizes the experience gained over many years of continuous autopilot design. The authors using this method[3,4,6,11] use one or a combination of discrete approximation techniques (reviewed recently by Slater[12]) to transform the resulting continuous compensation into a discrete compensation. The effect of the approximation in the design is typically checked by a precise simulation. Design using the second category includes the w-plane techniques,[7,8] z-plane Nyquist techniques,[9] and the discrete state space techniques of Berman,[5] Johnson,[11] and the authors of this paper. The purpose here is not to recommend any one particular design method; however, the approximations inherent in the category 1 methods introduce an additional constraint which may be important in sample rate selection. It is interesting to note that all authors reporting the use of a category 1 design method selected a sample rate which was a higher multiple of the bending modes of interest than those authors using a category 2 method.

The selection of an appropriate sample rate for an aircraft digital controller is a compromise among many factors. Factors which provide incentive to lower the sample rate (ω_s) are cost and accuracy. By lowering ω_s, the cost of A/D and D/A equipment is directly reduced. The lower CPU % time usage could be utilized for additional functions or could be translated into reduced central processor costs. The increased accuracy obtained by slower sampling is well documented[3] and can also be translated into cost savings by reducing the word size. These economic arguments indicate that the best engineering choice is the slowest possible sample rate which meets all performance specifications.

Factors which provide a lower limit or incentive to increase the sample rate are: 1) closed-loop bandwidth or time response requirements; 2) sensitivity to parameter variations; and 3) effect of random disturbances. If using category 1 type design methods, the approximation in the design would provide an additional artificial lower limit on the sample rate which may, depending on the factors above, influence the sample rate. However, this factor will not be discussed since it can be removed by changing one's design method.

II. Closed-Loop Bandwidth/Time Response

This consideration is the absolute lower bound to the sample rate and has a theoretical basis in the sampling theorem

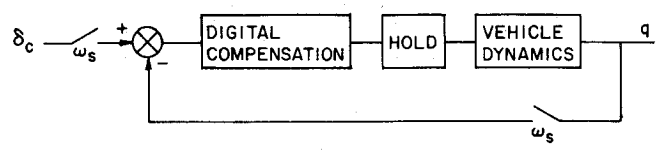

Fig. 1 Single autopilot channel schematic.

Presented as Paper 74-885 at the AIAA Mechanics and Control of Flight Conference, Anaheim, California, August 5-9, 1975; submitted August 26, 1974; revision received February 3, 1975. This work was partially supported by NASA Flight Research Center under Grant NSG-4002.

Index categories: Aircraft Handling, Stability and Control; Computer Technology and Computer Simulation Techniques; Navigation, Control and Guidance Theory.

*Assistant Professor of Aeronautics and Astronautics. Member AIAA.

†Research Engineer. Student Member AIAA.

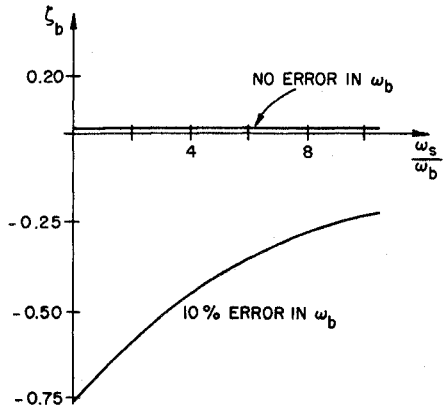

Fig. 2 Closed-loop bending mode damping vs ω_s.

developed by Shannon.[13] Assuming we can represent an autopilot function by a single channel as depicted in Fig. 1, the performance can be specified in terms of the frequency response of q vs δ_c. The sampling theorem states that in order to reconstruct an unknown continuous signal from samples of that signal, one must use a sample rate which is twice as high as the highest frequency contained in the unknown signal. This theorem applies to a feedback controller such as Fig. 1 because δ_c is an unknown signal whose information up to a given frequency must be extracted if the system output (q) is to follow δ_c up to that given frequency of "bandwidth." The sample rate, therefore, must be at least twice the required closed-loop bandwidth of the system.

It is important to note the distinction between the closed-loop bandwidth and the frequencies in the open loop vehicle dynamics since these two frequencies can be quite different in aircraft autopilots. Specifically, closed-loop bandwidths are typically less than 2 HZ whereas important open-loop bending and slosh mode frequencies are typically 2-10 Hz or even higher. For stability reasons, it is important to be able to distinguish between rigid body motion and vehicle resonances. Information concerning the state of the vehicle resonances can be extracted from sampling the vehicle output (q in Fig. 1) without satisfying the sampling theorem because some a priori knowledge is available (albeit imprecise) concerning these dynamics. This a priori knowledge of the dynamic model of the vehicle can be included in the compensation in the form of a notch filter if using classical design or as part of the observer dynamics if using state space methods. The question that immediately arises, however, is: how accurately must these high-frequency dynamics be known? This is an important question and is treated in the following section as a separate issue in the selection of sampling rates.

The "closed-loop bandwidth" limitation provides the fundamental lower bound on the sample rate. In practice, however, the theoretical lower bound of twice the bandwidth would not be judged sufficient in terms of desired time responses. For a system with a rise time on the order of 1 sec[3,4] and a closed-loop bandwidth on the order of 0.5 Hz it is not unreasonable to insist on a sample rate of 5 or 10 Hz which is a factor of 10 or 20 times the closed-loop bandwidth. Since pilot input is sampled and often passed directly into a low-pass filter, a one or two sample period delay is possible between pilot input and actuator command. This factor alone suggests that the sample period be kept a small fraction of the rise time, in line with the suggestion of a 10 Hz sample rate for a 1 sec rise time.

In summary, the sampling theorem provides a theoretical lower bound that ω_s must be twice the closed-loop bandwidth. This criterion has nothing to do with the vehicle resonances, which affect ω_s only through their uncertainty. In practice, ω_s would probably be selected to be 10 or 20 times the bandwidth.

III. Sensitivity to Parameter Variations

Any control design relies to some extent on knowledge of the parameters representing plant dynamics. Discrete systems exhibit an increasing sensitivity for a decreasing ω_s when the sample interval becomes comparable to any of the open-loop vehicle dynamics. No guidelines are known which provide an easily applied procedure for determining an acceptable sample rate vs. expected parameter uncertainties; however, we have studied the closed-loop pole movement with an error in a high frequency vehicle resonance. In this section we will: a) briefly outline the design method used to arrive at the various sensitivity and performance information; b) demonstrate the sensitivity of an autopilot including short period dynamics with imperfect knowledge of the first bending frequency; and c) reduce the sensitivity of the example by modifying the designs.

Basic Relations

The discretized closed-loop system consists of the plant

$$x_{i+1}=\phi_p x_i+\Gamma_p u_i+w_i \quad y_i=H x_i+v_i \tag{1}$$

where x_i is the state vector, u_i is the control, w_i is white disturbance noise, y_i is the measurement vector, and v_i is the white measurement noise. The compensator is

$$\left.\begin{aligned}\hat{x}_i&=\bar{x}_i+K(y_i-H\bar{x}_i)\\ \bar{x}_{i+1}&=\phi\hat{x}_i+\Gamma u_i\end{aligned}\right\}\ \text{the observer} \tag{2}$$

$$u_i=C\hat{x}_i \ \text{ the controller} \tag{3}$$

where $\bar{x}_i$ is the estimated value of the state before the measurement y_i has been performed and $\hat{x}_i$ is the estimated value of the state after the measurement.

If the mechanized model in the observer is identical to the plant, then the estimate error, defined to be

$$\tilde{x}=\hat{x}-x \tag{4}$$

goes to zero[14] with roots given by the observer characteristic equation

$$|\phi(I-KH)-Iz|=0 \tag{5}$$

where I is the unit matrix and the total closed-loop system roots are given by the controller and the observer roots, i.e. of the polynomial

$$|\phi+\Gamma C-Iz|\ |\phi(I-KH)-Iz|=0 \tag{6}$$

If $\phi_p\neq\phi$ and $\Gamma_p\neq\Gamma$, the plant-compensator system becomes

$$\begin{aligned}x_{i+1}&=\phi_p x_i+\Gamma_p C\hat{x}_i+w_i\\ y_i&=Hx_i+v_i\\ \hat{x}_{i+1}&=(I-KH)\ (\phi+\Gamma C)\hat{x}_i\\ &\quad+KH(\phi_p x_i+\Gamma_p C\hat{x}_i+w_i)+Kv_i\end{aligned} \tag{7}$$

and the characteristic equation is

$$\begin{bmatrix}\phi_p-Iz & \Gamma_p C\\ KH\phi_p & (I-KH)\ (\phi+\Gamma C)+KH\Gamma_p C-Iz\end{bmatrix}=0 \tag{8}$$

The separation of controller and observer roots no longer exists and Eq. (8) must be solved to obtain the system roots.

For the sensitivity analysis we will use discrete synthesis of a steady-state optimal linear regulator and observer. This com-

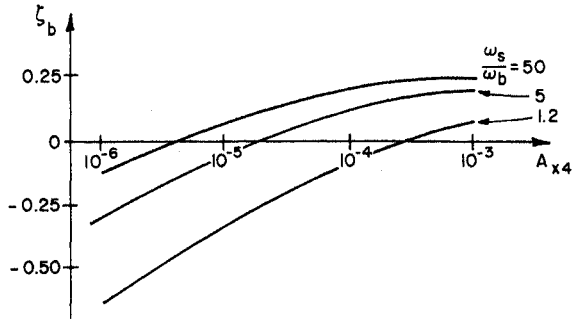

Fig. 3 Closed-loop bending mode damping vs A_{x4}, weighting factor (10% ω_b error).

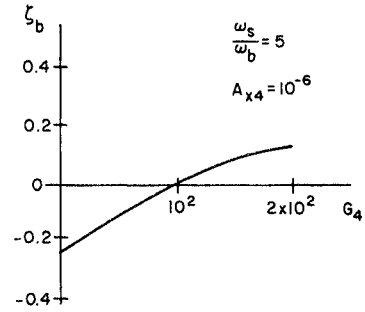

Fig. 4 Closed loop bending mode damping vs noise magnitude, G_4 (10% ω_b error).

putational scheme calculates the optimal full-state variable feedback $u_i = Cx_i$ which minimizes the quadratic cost function

$$J = \sum_{i=o}^{\infty} (x_i^T A x_i + u_i^T B u_i) \tag{9}$$

(where A is the weighting matrix of the states and B is the weighting matrix of the controls) and calculates the gains for the optimal linear discrete observer which minimizes the estimation error given the noise statistics. The computational algorithm is based on the discrete eigenvector decompositon proposed by Vaughan[15] and the numerical method of solution by Bryson and Hall[16] for synthesis of optimal continuous systems. To evaluate the effect of parameter errors on the root locations in the system designs, Eq. (8) is solved directly.

Example

The aircraft used as an example is a hypothetical one used in a recent study.[3,4] The model is for the longitudinal short period motion and is represented by a fourth-order system including the rigid body mode and the first bending mode. At zero altitude and Mach 1.2 the open loop rigid body poles are located[3] at $s = -2 \pm j13.5$ rad/sec. The bending mode is lightly damped ($\zeta_b = 0.01$) with a natural frequency, ω_b, of 4 Hz. The closed-loop poles of the rigid body were relocated by the optimal discrete analysis to $s = 16 \pm j10$ with essentially no change in the bending mode poles.

It can be shown[17] that the optimal compensator (controller plus observer) generates a very deep and narrow notch filter which filters out the unwanted bending frequencies. The width of the notch filter is directly related to the low damping of the bending mode and the noise properties of the system. Furthermore, the optimal observer gains for the bending mode are very low causing low damping in this estimation error mode. If the bending frequency of the vehicle varies from the assumed bending frequency, the incoming bending frequency misses the notch and is transmitted as a positive feedback to the elevator. This is demonstrated in Fig. 2 as a function of sample rate, ω_s. Note the insensitivity to sample rate for perfect knowledge of the bending mode and the strong influence of sample rate for the 10% error case. For this particular case the bending modes were unstable for all sample rates with a 10% ω_b error, indicating a very sensitive system which is typical of so-called optimal observer designs based solely on noise statistics.

The sensitivity can be reduced by increasing the width of the notch through variations of the weighting factors in Eq. (9) that apply to the bending modes and by introducing additional disturbance noise in the bending mode state of Eq. (1) Figure 3 shows the effect on ζ_b due to the bending mode weighting factor A_{x4} and demonstrates a substantial reduction in sensitivity. Note that it is possible to have $\zeta_b > 0.05$ with a 10% ω_b error and a sample rate only 20% faster than the bending mode. Figure 4 depicts a similar trend for the parameter (G_4) representing the magnitude of the disturbance noise on the bending mode state. Ultimately, a final design would consist of the combination of A_{x4}, G_4 and possibly other currently unidentified constants which yield the "best" performance in terms of sensitivity, noise response, and rigid body response.

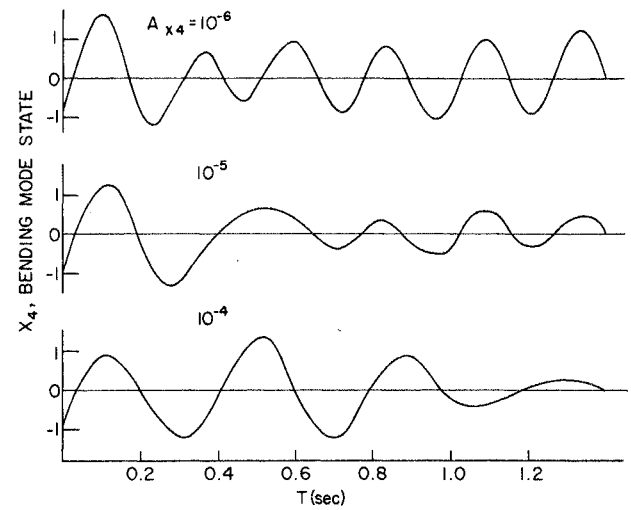

Fig. 5 Bending mode time history for various weighting factors (10% ω_b error). $\omega_s/\omega_b = 1.2$ ($T = 0.2$ sec), $G_4 = 100$.

Since this discrete analysis was based only on behavior at the sample points, a simulation of the autopilot designs was performed on a digital computer which included calculations of the continuous vehicle behavior between sample points. Figure 5 is a time history of the bending mode state (excluding all rigid body motion) as excited by an impulsive wind gust. It generally verifies that the intersample behavior is predicted adequately by the discrete analysis of Figs. 3 and 4.

Summary

The system becomes increasingly sensitive to bending mode frequency errors as the sample rate decreases; however, for perfect frequency information, there is no effect of sample rate on bending mode damping. Designs were demonstrated that yielded good bending mode damping with a 10% ω_b error and a sample rate 20% faster than the bending mode. Since a typical rise time requirement for this type of autopilot would be on the order of 1 sec, an adequate closed-loop response would require a sample rate on the order of 10 Hz. This sensitivity example was based on one bending mode at 4 Hz and, in this case, sensitivity considerations would not impose a higher sample rate requirement. However, sensitivity of the system to off nominal vehicle parameters must be evaluated and, especially in slow sample rate cases, the system should be specifically designed to minimize the sensitivity.

IV. Effect of Random Disturbances

The behavior of a continuous system driven by white or colored noise is well understood and is described in various

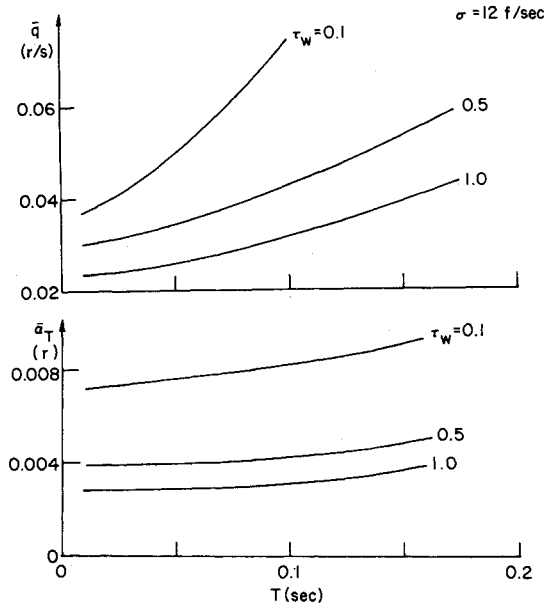

Fig. 6 Root mean square response vs T at various τ_w.

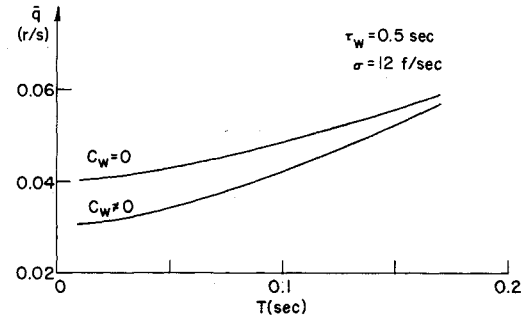

Fig. 7 Effect of wind state feedback on rms response.

sources.[18-20] The rms response will depend on dynamic characteristics of the closed-loop system and on correlation times of the colored noise. For a discrete controller, the system exhibits an increasing noise response as the sample rate decreases.

Basic Relations

For the addition of colored noise, we modify Eq. (1) by augmenting the state and obtain

$$\begin{bmatrix} x \\ w \end{bmatrix}_{i+1} = \phi \begin{bmatrix} x \\ w \end{bmatrix}_i + \Gamma u_i + \Gamma_n \mu_i$$

$$y_i = H \begin{bmatrix} x \\ w \end{bmatrix}_i + v_i \qquad (10)$$

where w_i is the Gauss-Markov sequence driven by white noise μ_i with covariance $Q_D \delta_{ij}$. Algorithms for the computation of Q_D given the continuous noise statistics are given in Ref. 17.

If full-state feedback is used for control and an optimal observer reconstructs the states, then the steady state covariance matrix of the states, X, is given by[18]

$$X - M = (\phi + \Gamma C)\ (X - P)\ (\phi + \Gamma C)^T \qquad (11)$$

where M and P are the steady state covariance matrices of the observer errors before and after the measurements, respectively. The square roots of the elements on the diagonal of X are the rms values of the states.

The controller, $u_i = C\hat{x}_i$, uses the fact that the external disturbance w_i is not completely random (or white) noise. When the disturbance is modeled as a first-order Gauss-Markov process, as we have done here, the disturbance is characterized by its correlation time, τ_w.

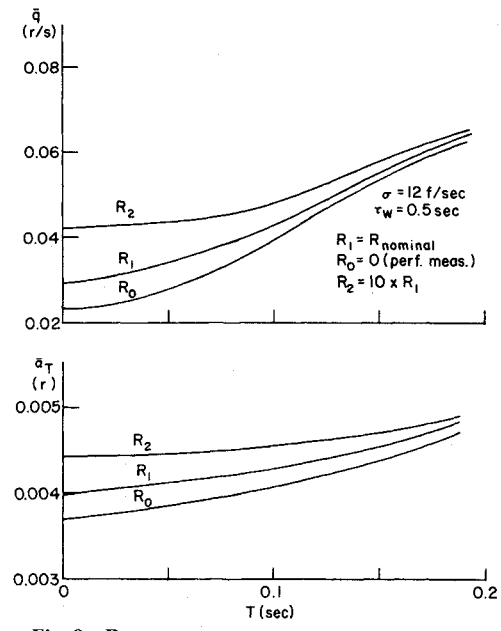

Fig. 8 Root mean square vs measurement errors.

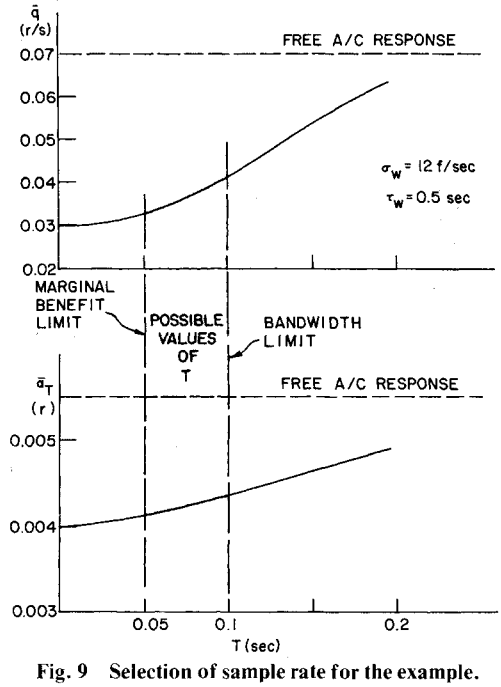

Fig. 9 Selection of sample rate for the example.

Example

Using the short period dynamics[3] at Mach 1.2 and zero altitude as in the previous example, we evaluated the rms response of pitch rate, $\bar{q}$, and the total angle of attack $\bar{\alpha}_T$ (including that portion generated by the gust) due to a vertical wind gust with an rms value,[3] σ, of 12 fps and measurement errors of $\sigma_q = 0.33°$/sec for the rate gyro and $\sigma_a = 0.7$ fps^2 for the accelerometer. In order to maintain the intensity (or energy) of the wind constant, the power spectral density, Q, was adjusted with the correlation time by

$$Q = 2\sigma^2/\tau_w \qquad (12)$$

Figure 6 shows the response of q and α_T vs sample rate at different correlation times around the nominal τ_w of 0.5 sec.[3]

The effects of sample rate are most pronounced when the correlation time is on the same order as the sample interval, T $(=1/\omega_s)$. For correlation times long compared to T, there is essentially no dependence on sample rate. In addition to showing the effect of T, Fig. 6 emphasizes the importance of τ_w on the rms response of discrete controllers.

As a demonstration of the value of state space design methods, we have included Fig. 7 to compare the wind response of a system with feedback from the estimated wind state, $C_w \neq 0$, and no wind state estimate feedback, $C_w = 0$. Although the figure does not indicate an overwhelming improvement by the extra feedback, the 20% improvement may be significant in some cases.

The total rms response is due to both wind effects and measurement error effects. Since our purpose is to pick the sample rate as slow as possible, Fig. 8 has been included to show the effect that measurement instrument quality would have on this selection. From a total systems standpoint, it theoretically could be more cost effective to use higher quality measurement devices than to increase the sample rate and digital system costs; however, for this example no significant reduction in sample rate is possible by decreasing the nominal sensor errors.

Figure 9 is a repeat of the previous nominal response data with additional information concerning the sample rate selected by closed-loop bandwidth considerations and the rms response of the aircraft with no control. Since one of the purposes in adding the controller was to improve the gust response, the A/C free response adds perspective in what is being accomplished with the controller. Although no gust alleviation specification was stated in the previous autopilot studies,[3,4] it is desirable to provide as much as possible. With sample rate at the 10 Hz ($T=0.1$) value determined by bandwidth considerations, 75% gust alleviation of that possible with continuous control is achieved. By increasing the sample rate to 20 Hz ($T=0.05$ sec), 90% of the achievable gust alleviation is achieved. Whether the extra gust alleviation is worth the doubling of computation requirements for the algorithms involved is a matter of judgment.

Summary

Techniques are well established to evaluate random disturbances on a digitally controlled system. The study of the effects on the example showed that it might be desirable to increase the sample rate from the 10 Hz value determined by bandwidth considerations to 20 Hz. No appreciable advantage is apparent from raising it any higher than 20 Hz.

V. Conclusions

The sample rate should be selected based on three criteria: 1) closed-loop rigid body time response (or bandwidth); 2) sensitivity to vehicle parameter uncertainties, especially vehicle resonance frequency undertainties; and 3) response to random disturbances such as wind gusts. Stabilization of vehicle resonances can be accomplished theoretically at any sample rate, but the controller becomes unacceptably sensitive to parameter uncertainties as the sample rate approaches the important vehicle resonance frequencies.

The concepts above were applied to the longitudinal dynamics including one bending mode of a hypothetical aircraft at $M=1.2$ and zero altitude. For this example, 1) the time response criterion suggested a sample rate of about 10 Hz, 2) the system was easily modified to be insensitive to a 10% error in the bending mode frequency at a 10 Hz sample rate, and 3) the gust alleviation could be somewhat enhanced by increasing the sample rate to 20 Hz.

References

[1] Deets, D. A. and Szalai, K. J., "Design and Flight Experience with a Digital Fly-By-Wire Control System Using Apollo Guidance System Hardware on an F-8 Aircraft," AIAA Paper 72-881, Stanford, Calif., 1972.

[2] Mathews, M. A., "SAAB Digital Flight Control," AIAA Paper 74-26, Washington, D.C., 1974.

[3] Borow, M. S., et al., "Navy Digital Flight Control System Development," Honeywell Document No. 21857-FR, Honeywell, Inc., Minneapolis, Minn., Dec. 1972.

[4] Sutton, M. L., "Feasibility Study for an Advanced Digital flight Control System," LSI Tech. Rept. ADR-773, Lear-Siegler, Inc., Santa Monica, Calif., Oct. 1972.

[5] Berman, H. and Gran, R., "An Organized Approach to the Digital Autopilot Design Problem," *Journal of Aircraft*, Vol. 11, July 1974, pp. 414-422.

[6] Osder, S., "Digital Autopilots: Design Considerations and Simulator Evaluations," NASA Ames Research Center, Pub. 70-1364-00-00, Oct. 1971.

[7] Lee, J. F. L., "A Digital Flight Control System Design Approach for a Space Shuttle Booster Type Vehicle," AIAA Paper 74-20, Washington, D.C., 1974.

[8] Stubbs, G. S., Oenchuk, A., and Schlundt, R. W., "Digital Autopilots for Thrust Vector Control of the Apollo CSM/LM Vehicles," AIAA Paper 69-847, Princeton, N.J., 1969.

[9] Simmons, J. C. and Hall, B. M., "Digital Control System Development for the Delta Launch Vehicle," AIAA Paper 73-847, Key Biscayne, Fla. 1973.

[10] Johnson, J. M., "The Application of Digital Filters Using Observers to the Design of an ICBM Flight Control System," *Journal of Spacecraft and Rockets*, Vol. 11, July 1974, pp. 498-504.

[11] Edwards, J. W., "Flight Test Experience in Digital Control of a Remotely Piloted Vehicle," AIAA Paper 72-883, Stanford, Calif., 1972.

[12] Slater, G. L., "A Unified Approach to Digital Flight Control Algorithms," AIAA Paper 74-884, Anaheim, Calif., 1974.

[13] Ragazzini, S. P. and Franklin, G. F., *Sampled Data Control Systems*, McGraw-Hill, New York, 1958.

[14] Bryson, A. E. and Luenberger, D. G., "The Synthesis of Regulator Logic Using State Variable Concepts," *IEEE Proceedings*, Vol. 58, Nov. 1970, pp. 1803-1811.

[15] Vaughan, D. R., "A Non-recursive Solution of the Discrete Matrix Riccati Equation," *IEEE Transactions on Automatic Control*, Oct. 1970.

[16] Bryson, A.E. and Hall. W.E., "Optimal Control and Filter Synthesis by Eigenvector Decomposition," SUDAAR Rept. 436, Nov. 1971, Stanford University, Stanford, Calif.

[17] Katz. P. and Powell, J.D., "Selection of Sampling Rate for Digital Control of Aircraft," SUDAAR Report No. 486, Sept. 1974, Aero & Astro Dept., Stanford University, Stanford, Calif.

[18] Bryson, A. E. and Ho, Y, C., *Applied Optimal Control*, Ginn-Blaisdell, Waltham, Mass., 1969.

[19] Bryson, A. E., "Control Theory for Random Systems," SUDAAR Rept. 447, Sept. 1972, Stanford University, Stanford, Calif.

[20] Kwakernaak, H. and Sivan, R., *Linear Optimal Control Systems*, Wiley-Interscience, New York, 1972.